

Experimental Evaluation of Moving Target Compensation in High Time-Bandwidth Noise Radar

Martin Ankel^{*1,2}, Robert S. Jonsson^{1,2}, Mats Tholén^{3,4}, Tomas Bryllert^{1,2}, Lars M.H. Ulander⁵, Per Delsing¹

¹Department of Microtechnology and Nanoscience, Chalmers University of Technology, Sweden

²Research and Concepts, Surveillance, Saab, Sweden

³Nanostructure Physics, KTH Royal Institute of Technology, Sweden

⁴Intermodulation Products AB, Sweden

⁵Department of Space, Earth and Environment, Geoscience and Remote Sensing, Chalmers University of Technology, Sweden

*ankel@chalmers.se

Abstract—In this article, the effect a moving target has on the signal-to-interference-plus-noise-ratio (SINR) for high time-bandwidth noise radars is investigated. To compensate for cell migration we apply a computationally efficient stretch processing algorithm that is tailored for batched processing and suitable for implementation onto a real-time radar processor. The performance of the algorithm is studied using experimental data. In the experiment, pseudorandom noise, with a bandwidth of 100 MHz, is generated and transmitted in real-time. An unmanned aerial vehicle (UAV), flown at a speed of 11.5 m/s, is acting as a target. For an integration time of 1 s, the algorithm is shown to yield an increase in SINR of roughly 13 dB, compared to no compensation. It is also shown that coherent integration times of 2.5 s can be achieved.

Keywords—Doppler Tolerance, Experimental Long Time Coherent Integration, Noise Radar, Stretch Processing

I. INTRODUCTION

The military surveillance radar is a crucial piece of equipment in the modern battlefield, but it is expensive and vulnerable and, therefore, it must be heavily protected, especially as modern lightweight electronic warfare sensors make precise and fast localisation of radar systems possible. Hence, methods and techniques of protecting the radar system is of high interest. One way to protect the radar system is to reduce the risk of the transmitted signal being intercepted in the first place, e.g., low probability of intercept (LPI) radar [1], [2].

To achieve LPI it is desirable to transmit a waveform with low spectral power density, i.e., the radar should transmit continuously with high instantaneous bandwidth and preferably integrate for an extended period of time. A type of radar that generally operates under these conditions is the noise radar [3]–[6]. Introducing randomness to the waveform makes it robust against intelligent jamming and, even if detected, the information revealed is limited. For example, the radar mode of operation is difficult to deduce, since the pulse repetition frequency is not revealed as it would be in most other types of radar systems. Additionally, noise radars are unambiguous in range and Doppler [4], [5].

The combination of high bandwidth and long integration time will lead to significant cell migration of a moving target

during the coherent processing interval (CPI) and a reduction in SINR. As an example, with a bandwidth of 100 MHz and a target moving at 10 m/s the maximum coherent integration time is 150 ms. To integrate for longer times, the movement of the target has to be accounted for. This can be done in the correlation processing by either compressing or expanding the reference signal, a method referred to as stretch processing [7]–[12]. It should be mentioned that, while the velocity and acceleration of targets can be adequately accounted for, there may be other sources of coherence loss that limit the coherent integration time.

The article is organised as follows. Section II discusses the Doppler tolerance of noise radars and details a stretch processing algorithm tailored for batched processing of the noise signal. The experimental results are presented and discussed in Section III. Finally, the conclusions are given in Section IV.

II. THEORY VELOCITY COMPENSATION

Noise radars generate and transmit a random or pseudo-random noise signal. Detection is performed by the concept of matched filter, which is implemented by performing a convolution between the received signal, y , and the reference signal, x , as

$$R[k] = \sum_n y_n x_{n-k}^*, \quad (1)$$

where the subscript denotes discrete samples of the respective signals. A correlation detector contains the function $|R[k]|^2$ which will exhibit peaks at indices corresponding to strong correlations between the signal and the reference, indicating a reflection corresponding to that delay. The magnitude of the peak depends on the similarity of x and y , meaning any distortion of y will result in a correlation loss and reduce the radar's detection performance. One such distortion is due to the movement of a target.

We assume that a target at a distance R_0 is moving with constant radial velocity v_s . The received signal at time t is proportional to the reference delayed by $2(R_0 - v_s t)/c$, where c is the speed of light. If the distance covered by the target during a CPI is insignificant in relation to the range resolution,

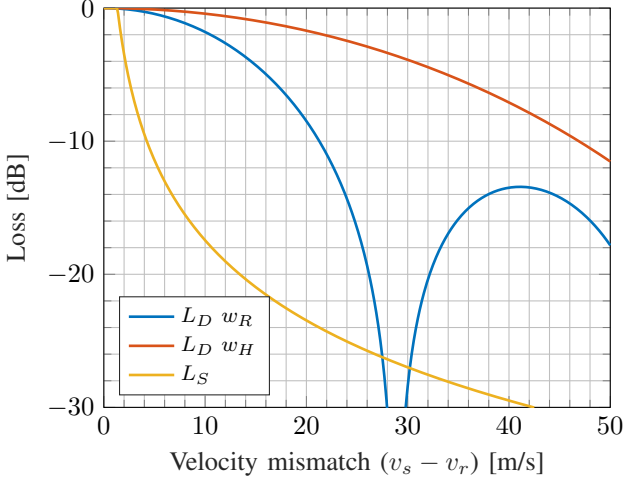


Fig. 1. Theoretical Doppler loss (L_D), for a rectangular window (w_R) and a Hann window (w_H), and theoretical cell migration loss (L_S) as a function of velocity mismatch between the reference and signal. The losses are calculated for a carrier frequency of 1.3 GHz, a batch length of 4 ms, a bandwidth of 100 MHz, a sampling rate of 125 MHz and a CPI length of 1 s.

only the Doppler shift has to be accounted for, and the term $2v_s t/c$ can be ignored. However, if the covered distance matters, stretch processing has to be considered. These two cases will be treated separately and referred to as *Doppler Compensation* and *Stretch Compensation*, respectively.

A. Doppler Compensation

Compensating for the Doppler shift is performed by applying a Doppler modulation to the reference signal as

$$x'_n = x_n \cdot e^{-2\pi i(2v_r f_c/c) \cdot \frac{n}{f_s}}, \quad (2)$$

where v_r is the reference velocity, f_s is the receiver's sampling rate and f_c is the carrier frequency. If v_r is close to the target velocity, the loss due to the movement of the target is mitigated. In a real world application the target velocity is not known to the radar and must be guessed. Performing a calculation for every possible velocity would be extremely resource demanding. A more efficient approach is to compute the correlations on a grid of different velocities spaced by δv , where δv should be selected such that the maximum Doppler loss does not exceed a specified threshold.

The correlation loss due to a Doppler shift for noise radars has been investigated in [13] and it was found that the loss primarily depends on the window function $w(t)$ as

$$L_D = \left| \mathcal{F}(w(t)) \right|^{-2}. \quad (3)$$

For example, for a rectangular window the loss is

$$L_D = \left| \frac{\sin[2\pi f_c(v_s - v_r)t_p/c]}{2\pi f_c(v_s - v_r)t_p/c} \right|^{-2}, \quad (4)$$

where t_p is the batch length. To get an idea of the velocity spacing required we simulate the loss at L-band (1.3 GHz) in Fig. 1, for a rectangular window as well as a Hann window, with

$t_p = 4$ ms. In this case, if 3 dB loss is acceptable, δv would be roughly 26 m/s for a rectangular window and 53 m/s for a Hann window. It should be kept in mind that a Hann window also decreases the signal to noise ratio with approximately 1.8 dB. The δv spacing basically scales linearly with batch length, meaning shorter batches of 0.4 ms and 40 μ s would have a required spacing of 260 m/s and 2600 m/s, respectively, for a rectangular window.

B. Stretch Compensation

Typically, in order to calculate the range-Doppler map for a noise waveform in an efficient manner, batched processing is preferred [14], especially for real-time implementation on, e.g., a field programmable gate array (FPGA). Therefore, it is desirable to implement the stretch compensation in conjunction with the batched operation, while simultaneously keeping the number of extra operations to a minimum and avoiding the need to buffer data.

Here, we present an algorithm that efficiently performs an approximate stretch processing by applying a constant phase factor per batch [11], [12]. Assume that the CPI consists of N samples, labelled by index $n = 0, 1, \dots, N - 1$, and that the Doppler shifted reference signal, x'_n in (2), is segmented into P batches, each batch containing $M = N/P$ samples covering a time of t_p . Let each batch populate a row in a matrix, $\mathbf{x}'_{p,m}$, of size $P \times M$ and form the discrete Fourier transform of each respective row, as

$$\mathbf{X}_{p,q} = \frac{1}{M} \sum_{m=0}^{M-1} \mathbf{x}'_{p,m} e^{-2\pi i \frac{q \cdot m}{M}}. \quad (5)$$

If the distance the target moves during the time t_p is negligible with respect to the range resolution, stretching over each individual batch is unnecessary. In this case it is sufficient to perform time translation only in slow time, i.e., between batches. This can be done in the frequency domain, utilising the Fourier transform property that $\mathcal{F}[f(n-a)] = \mathcal{F}[f(n)] e^{-\frac{2\pi i}{N} ka}$. Between batches, the reference is shifted with the factor $a = 2v_r f_s t_p / c$ to compensate for target motion, as

$$\mathbf{X}'_{p,q,r} = \mathbf{X}_{p,q} e^{-2\pi i \frac{q \cdot p}{M} \frac{2v_r f_s t_p}{c}} = \mathbf{X}_{p,q} e^{-2\pi i q \cdot p \frac{2v_r}{c}}, \quad (6)$$

where $p = 0, 1, \dots, P - 1$ is the batch index and where we have utilised the fact that $t_p = M/f_s$.

The range-Doppler map is calculated by performing the cross-correlation in the frequency domain and then taking the Fourier transform of each column, i.e.,

$$\mathbf{R}_{l,m,r} = \sum_{p=0}^{P-1} \left(\sum_{q=0}^{M-1} \mathbf{Y}_{p,q} (\mathbf{X}'_{p,q,r})^* e^{2\pi i \frac{q \cdot p}{M}} \right) e^{-2\pi i \frac{l \cdot p}{P}}. \quad (7)$$

This processing is efficiently implemented with the Fast Fourier Transform algorithm. There are only two additional operations required by the algorithm to perform the stretch compensation: calculation of one phase factor for each sample and one element-wise multiplication. In FPGA terms this would consist of a cosine block, a sine block and two product blocks (and some counters), making it easy to implement and relatively resource

efficient. Such an implementation is also practical considering data does not have to be buffered, but can be continuously streamed.

The spacing of the different stretch hypotheses dv can be determined by requiring a maximum allowable stretch loss L_S , given by [12]

$$L_S = 4(v_s - v_r)^2 T_{\text{int}}^2 f_s B / c^2, \quad (8)$$

where T_{int} is the integration time. The migration loss as function of velocity mismatch can be seen in Fig. 1, for $f_s = 125$ MHz, $T_{\text{int}} = 1$ s and $B = 100$ MHz. If 3 dB loss is considered to be acceptable, the required spacing is $dv = 1.9$ m/s. This is quite a dense grid that would require considerable computational resources. Luckily, there are several ways the calculations can be factorised to reduce the computational load, see e.g., [15].

In summary, it is important to keep track of both the Doppler loss (3) and the stretch loss (8) when designing the system and choosing δv and dv .

III. EXPERIMENTS AND RESULTS

In the experiments a pseudorandom sequence of 100 MHz bandwidth is generated and transmitted in real-time, at the L-band (1.3 GHz), by a digital microwave platform named Vivace [16]. Data is recorded with a software defined radio, capable of streaming data to disk drive storage at a rate of 250 MS/s. The equipment used is detailed in [17], with the only difference being that the transmitter's and receiver's FPGAs have been upgraded to handle continuous transmission and reception of non-repeating signals. Acting as a target is a DJI Matrice 600 UAV, flown in the direction of the antenna boresight at a speed of 11.5 m/s for 5 s.

Since this scenario consists of a monostatic continuous wave noise radar, there is significant self interference present, which is masking the target [18]. To be able to detect the UAV we processed the data with the Sequential CLEAN algorithm [17] to suppress strong clutter scatterers. When integrating the cleaned data over the entire recording with a batch time of $t_p = 4$ ms, we get the results shown in Fig. 2. The UAV is detectable with a maximum SINR of roughly 15.6 dB, where the 0 dB level is referenced to the average interference-plus-noise floor. As expected, there is significant broadening of the target signal in both range and Doppler.

The SINR is investigated with CPIs of 1 s for five different cases: no compensation, Doppler compensation (Sec. II-A), stretch compensation (Sec. II-B), Doppler and stretch compensation, and resampling of the reference waveform (i.e., true stretching). The resampling is performed over the entire CPI, but the CPI is still processed in batches. One could also consider the 2D correlator, which could potentially further increase the SINR at significant extra computational cost. The 5 s data is divided into five CPIs, with the results presented in Table 1, where the target signal strength is taken to be the strongest resolution cell. The performance of the approximative stretch algorithm is similar to the performance of full resampling. The effect that the different compensations has on the SINR in CPI 3 is illustrated in Fig. 3.

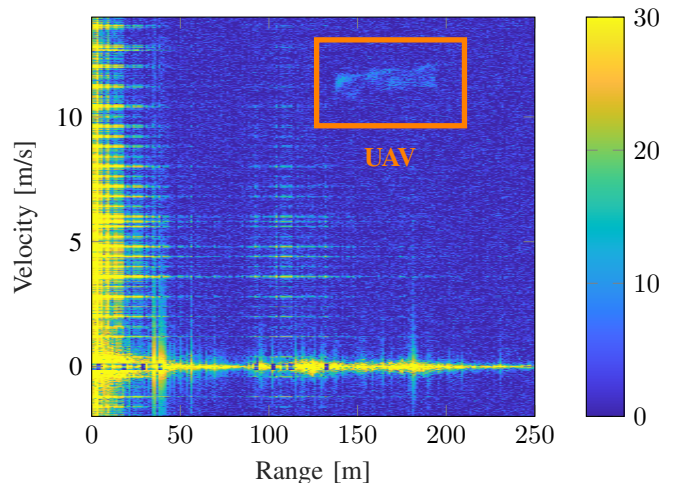


Fig. 2. Range-Doppler map of the entire, cluttered filtered, 5 s recorded sequence. The Doppler sidelobes are both due to spectral leakage from strong clutter scatterers (direct signal, ground returns, power lines, etc.) as well as due to spurious frequencies originating from the digital to analog converter. The UAV signal is highlighted by an orange box.

Table 1. SINR (dB) for different algorithms with 1 s CPI. The signal strength is taken to be the strongest resolution cell.

Compensation	CPI 1	CPI 2	CPI 3	CPI 4	CPI 5
None	18.9	16.2	16.8	15.0	15.5
Doppler	21.0	18.2	18.7	16.8	16.6
Stretch	28.2	23.2	26.1	23.5	24.7
Doppler & Stretch	29.7	23.2	30.4	27.1	28.7
Doppler & Resampling	29.8	23.2	29.5	27.7	28.1

The SINR processing gain is significant, yielding up to 13.6 dB improvement for CPI 3. Theoretically, without compensation the signal should spread uniformly in range and Doppler, if the target moves with constant velocity. In our case the spread is not uniform because the signal is relatively weak and effects from interference and noise become noticeable. If instead of the maximum, an average of the smeared target signal is used, the SINR increase is approximately 20 dB, which is in close agreement to the theoretical loss of $L_D + L_S = 2.4$ dB + 18.7 dB = 21.1 dB, see Fig. 1. It is not entirely clarified why CPI 2 performs worse than the rest, but a possible explanation is inconsistent flight speed, as the lightweight UAV is prone to wind disturbances. Indeed, close examination of CPI 2 reveals that the UAV accelerates, which is not compensated for by the algorithm.

When compensating for Doppler and cell migration, SINR gain as a function of integration time is investigated to estimate the coherence time of the UAV. The results are shown in Fig. 4, where a coherent integration time of up to 2.5 s is observed to be possible. We expect that several factors beside acceleration, such as multipath propagation and changes in aspect angle, impact the coherence time of the target.

IV. CONCLUSION

In summary, we have experimentally investigated moving target compensation for high time-bandwidth noise radars and

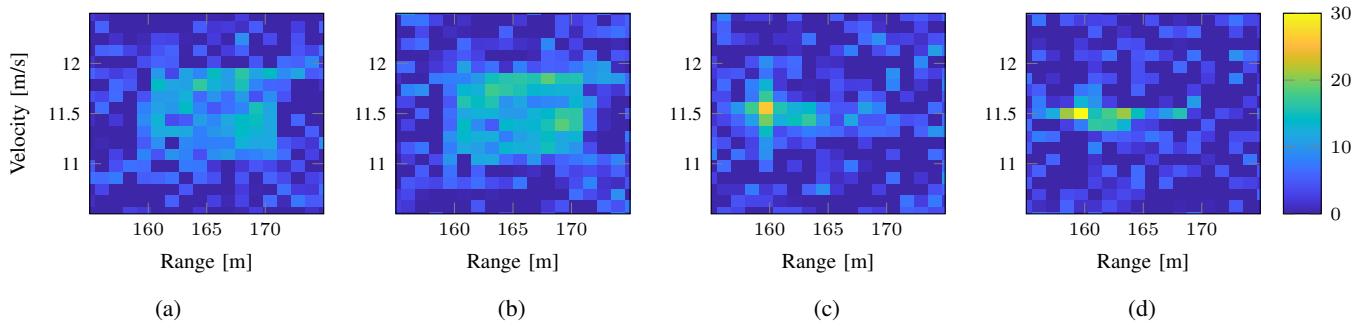


Fig. 3. UAV detection on CPI 3 with (a) **No compensation**: Maximum SINR of 16.8 dB. (b) **Doppler compensation**: Maximum SINR of 18.7 dB. (c) **Stretch compensation**: Maximum SINR of 26.1 dB. (d) **Doppler and stretch compensation**: Maximum SINR of 30.4 dB.

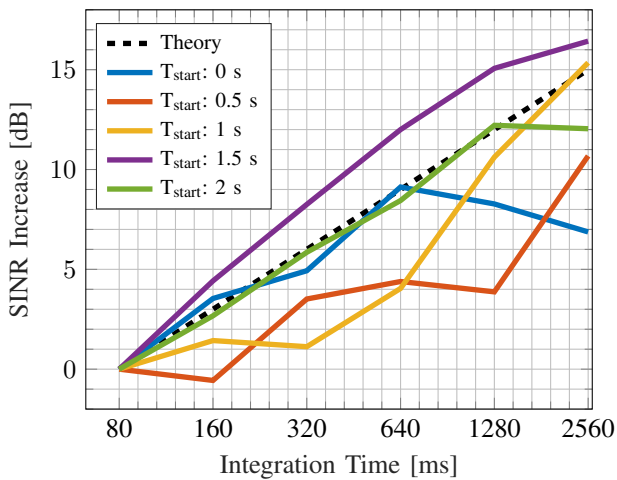


Fig. 4. SINR gain as a function of integration time for different sequences of the 5 s recorded data. The dashed black line illustrates the expected SINR increase of 3 dB increase per doubling of the integration time. The improvement is occasionally better than this, which can be explained by changes in straddling, aspect angle, multipath, etc.

shown that significant increase in SINR can be achieved by compensating for the Doppler shift and the target's cell migration. The coherence time of the target UAV fluctuates considerably, but times of at least 2.5 s are observed for a subset of the data. The compensation is performed using an approximative stretch algorithm suitable for real-time implementation. In future work, this algorithm will be implemented onto a real-time high time-bandwidth noise radar processor.

ACKNOWLEDGEMENT

The authors acknowledge support from the Knut and Alice Wallenberg (KAW) Foundation through the Wallenberg Centre for Quantum Technology (WACQT).

REFERENCES

- [1] A. G. Stove, A. L. Hume, and C. J. Baker, "Low probability of intercept radar strategies," *IEE Proceedings - Radar, Sonar and Navigation*, vol. 151, pp. 249–260, 2004.
- [2] P. E. Pace, *Detecting and classifying low probability of intercept radar*, 2nd ed. Norwood, MA, USA: Artech house, 2009.
- [3] B. M. Horton, "Noise-modulated distance measuring systems," *Proceedings of the IRE*, vol. 47, pp. 821–828, 1959.
- [4] M. Dawood and R. M. Narayanan, "Generalised wideband ambiguity function of a coherent ultrawideband random noise radar," *IEE Proceedings - Radar, Sonar, and Navigation*, vol. 150, pp. 379–386, 2003.
- [5] S. R. J. Axelsson, "Noise radar using random phase and frequency modulation," *IEEE Transactions on Geoscience and Remote Sensing*, vol. 42, pp. 2370 – 2384, 2004.
- [6] F. De Palo *et al.*, "Introduction to noise radar and its waveforms," *Sensors*, vol. 20, 2020.
- [7] W. J. Caputi, "Stretch: A time-transformation technique," *IEEE Transactions on Aerospace and Electronic Systems*, vol. AES-7, pp. 269–278, 1971.
- [8] T. L. Marzetta, E. A. Martinsen, and C. P. Plum, "Fast pulse Doppler radar processing accounting for range bin migration," in *The Record of the 1993 IEEE National Radar Conference*. Lynnfield, USA: IEEE, 1993, pp. 264–268.
- [9] K. S. Kulpa and J. Misiurewicz, "Stretch processing for long integration time passive covert radar," in *2006 CIE International Conference on Radar*. Shanghai, China: IEEE, 2006, pp. 1–4.
- [10] J. Xu *et al.*, "Radon-Fourier transform for radar target detection, I: Generalized Doppler filter bank," *IEEE transactions on aerospace and electronic systems*, vol. 47, pp. 1186–1202, 2011.
- [11] T. Shan *et al.*, "Efficient architecture and hardware implementation of coherent integration processor for digital video broadcast-based passive bistatic radar," *IET Radar, Sonar & Navigation*, vol. 10, pp. 97–106, 2016.
- [12] D. Bok, D. O'Hagan, and P. Knott, "Effects of movement for high time-bandwidths in batched pulse compression range-Doppler radar," *Sensors*, vol. 21, 2021.
- [13] C. Wasserzler, "Exploiting the low Doppler tolerance of noise radar to perform precise velocity measurements on a short set of data," *Signals*, vol. 2, pp. 25–40, 2021.
- [14] S. R. J. Axelsson, "Noise radar for range/Doppler processing and digital beamforming using low-bit ADC," *IEEE Transactions on Geoscience and Remote Sensing*, vol. 41, pp. 2703–2720, 2003.
- [15] L. M. H. Ulander, H. Hellsten, and G. Stenström, "Synthetic-aperture radar processing using fast factorized back-projection," *IEEE Transactions on Aerospace and Electronic Systems*, vol. 39, pp. 760–776, 2003.
- [16] Intermodulation Products AB, *Intermodulation Products – Vivace (2021)*, Segersta, Sweden, Accessed: May 17, 2023. [Online]. Available: <https://intermod.pro/products/microwave-platforms>
- [17] M. Ankel *et al.*, "Bistatic noise radar: Demonstration of correlation noise suppression," *IET Radar, Sonar & Navigation*, vol. 17, pp. 351–361, 2023.
- [18] S. R. J. Axelsson, "Analysis of random step frequency radar and comparison with experiments," *IEEE Transactions on Geoscience and Remote Sensing*, vol. 45, pp. 890–904, 2007.